Am J Cancer Res 2015;5(9):2660-2672
www.ajcr.us /ISSN:2156-6976/ajcr0013164

Original Article

Selective inhibition of EGFR downstream signaling reverses the irradiation-enhanced migration of HNSCC cells

Dominik Schuettler[1], Guido Piontek[1], Markus Wirth[1], Bernhard Haller[2], Rudolf Reiter[3], Gero Brockhoff[4], Anja Pickhard[1]

[1]Department of Otolaryngology Head and Neck Surgery, Technical University of Munich, Ismaninger Str. 22, Muenchen 81675, Germany; [2]Institute for Medical Statistics and Epidemiology, Technical University of Munich, Ismaninger Straße 22, Muenchen 81675, Germany; [3]Department of Otolaryngology Head and Neck Surgery, Section of Phoniatrics and Pedaudiology, University of Ulm, Prittwitzstr. 43, Ulm 89075, Germany; [4]Department of Gynecology and Obstetrics, University of Regensburg, Landshuter Str. 65, Regensburg 93053, Germany

Received July 20, 2015; Accepted July 29, 2015; Epub August 15, 2015; Published September 1, 2015

Abstract: Irradiation, which is one of the standard therapies used to treat squamous cell carcinoma of the head and neck (HNSCC), has been linked to enhanced tumor migration in carcinomas. In this study, we demonstrated that irradiation induced the phosphorylation of AKT, p38 MAPK and ERK. The combined activation of these pathways caused inactivation of GSK3β kinase, resulting in enhanced tumor cell migration. Here, we describe that the exclusive and specific inhibition of just one of the aforementioned key signaling molecules is sufficient to restore GSK3β activity and to reduce radiation-induced migration in HNSCC. These data indicate that pharmacological inhibition of pathways targeting GSK3β could decrease radiation-induced cell migration in HNSCC and thus potentially reduce metastasis and locoregional recurrence in patients.

Keywords: Radiation, migration, GSK3β

Introduction

HNSCC is the sixth most common cancer worldwide, with an estimated incidence of approximately 650,000 new cases and 350,000 cancer deaths per year [1]. Despite improvements in irradiation and chemotherapy regimens and the use of therapeutic antibodies, such as cetuximab, survival rates have slightly improved, with an overall survival of approximately 50% [2]. Local or regional recurrence at a previously irradiated tumor site is common in HNSCC, occurring in approximately 50% of patients within the first 5 years after receiving radiochemotherapy [3]. It has been demonstrated for both glioblastoma and HNSCC cell lines that sublethal irradiation promotes enhanced tumor cell migration, which is dependent upon epidermal growth factor receptor (EGFR) expression and signaling [4-6].

GSK3 was originally identified as a Ser/Thr kinase that inactivates glycogen synthase upon phosphorylation and thus regulates glucose metabolism [7]. Many additional functions have been reported, and GSK3 deregulation has been linked to various human disorders, such as Alzheimer's disease, diabetes and neoplasias [8]. It has been suggested that GSK3β plays a central role as a tumor suppressor in oral squamous cell carcinoma (OSCC). This molecule controls important signaling pathways and gene transcription. Therefore, it affects cell migration, proliferation, and apoptosis, and it is even involved in cellular transdifferentiation, which is known as epithelial-mesenchymal transition (EMT) [9]. For example, inhibition of GSK3β causes activated wnt-/β-catenin signaling, which has been linked to enhanced cell migration in OSCC [10]. GSK3β is negatively regulated through various pathways which, when activated, have been implicated in cancer promotion (**Figure 1**). Phosphorylation of GSK3β by AKT at the Ser9 residue inhibits its kinase activity [11]. Mutations in genes associated

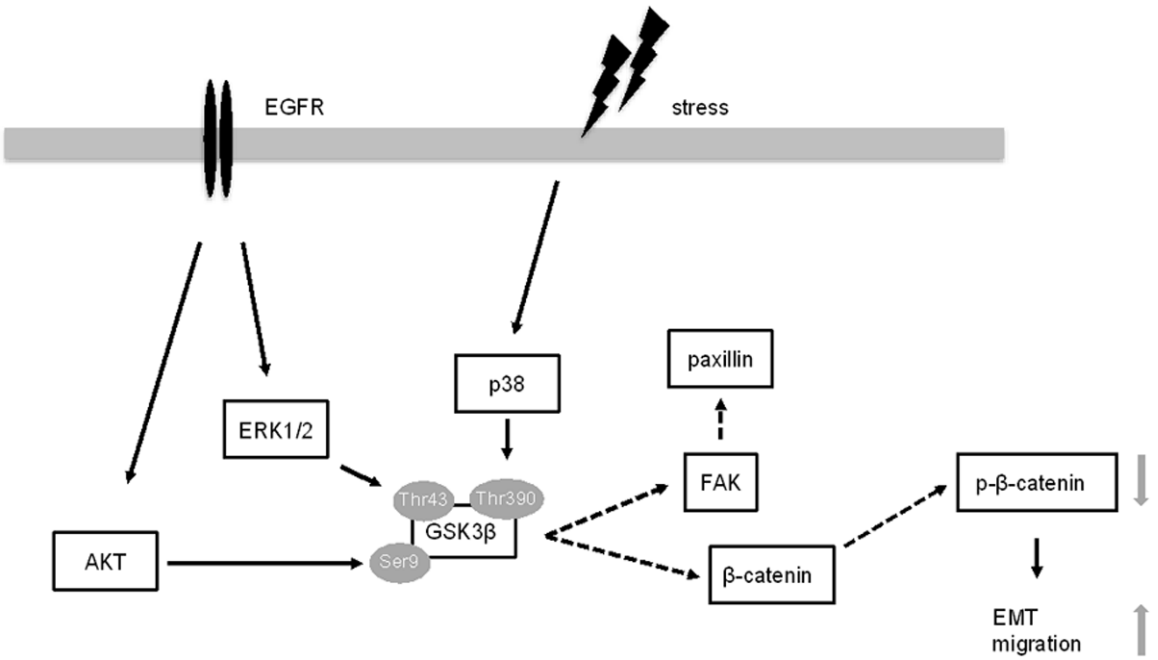

Figure 1. Model of the phosphorylation and inactivation of GSK3β. Activation of the EGFR downstream pathways AKT and ERK and stress-activated p38 MAPK leads to phosphorylation of GSK3β at three different amino acid residues. This combined phosphorylation results in GSK3β inactivation. Inhibited GSK3β is associated with non-phosphorylated FAK and paxillin, while activation of GSK3β leads to phosphorylation of FAK and paxillin. Additionally, activated, non-phosphorylated GSK3β is able to phosphorylate β-catenin at Ser33/37, resulting in the proteasomal degradation of β-catenin. GSK3β inactivation influences FAK and β-catenin, leading to increases in cell motility and migration.

with the PI3K-AKT-signaling pathway are common in HNSCC and are correlated with a more invasive phenotype [12]. Inhibition of GSK3β at the N-terminal Thr390 via stress-induced p38 MAPK has been demonstrated to lead to an accumulation of β-catenin [13]. Furthermore, ERK has been shown to associate with GSK3β, priming it for inactivation at Thr43, which leads to an up-regulation of β-catenin [14]. Dysregulation of ERK signaling is common in a variety of malignancies. Ras mutations, for example, occur in approximately 30% of all cancer types [15]. Stabilized β-catenin can act together with lymphoid enhancer-binding factor (LEF)/T-cell factor (TCF) to act as a transcription factor, affecting additional migration-promoting factors, such as myc, vascular endothelial growth factor (VEGF) and matrix metalloproteinases (MMPs) [10, 16]. Additionally, aberrant wnt signaling has been proposed to induce EMT [10]. β-catenin was originally identified as a molecule that links E-cadherin to the actin cytoskeleton [17]. Loss of membranous E-cadherin is considered to be a principle biochemical change that is indicative of EMT [18]. Based on these findings, Iwai et al. have concluded that accumulation of β-catenin leads to the redistribution of membranous E-cadherin, which induces EMT and promotes tumor migration [10]. In addition GSK3β can influence tumor migration via the targeting of molecules involved in cell-matrix adhesions, such as focal adhesion kinase (FAK) and paxillin [19] (**Figure 1**).

Here, we investigated the effects of irradiation on GSK3β-dependent tumor cell migration and analyzed relevant pathway (de-) activation as a function of ionizing irradiation.

Materials and methods

Cell culture

The human HNSCC cell lines Cal27 and HN were obtained from DSMZ (Braunschweig, Germany). UD-SCC-5 was obtained from the University of Dusseldorf (Otorhinolaryngology Clinic, Dusseldorf, Germany). Cells were cul-

tivated in Dulbecco's modified Eagle's medium (1× DMEM) (Gibco® Life Technologies, Carlsbad, CA, USA) with the addition of 10% fetal calf serum, 2 mM glutamine, 100 µg/ml penicillin and 100 U/ml streptomycin (all from Biochrom, Berlin, Germany). The cells were incubated under standard cell culture conditions (37°C containing 5% CO_2) until they reached 70% confluence.

Irradiation

For irradiation, a Gulmay Medical LTD RS225 X-Ray Box was used (Gulmay Medical, Surrey, United Kingdom). The irradiation was performed at the Department of Radiotherapy (Technical University of Munich) with 2 Gy or 10 Gy at 70 kV and 10 mA using filter #3 and a table height of 466 mm, resulting in a dose of approximately 1 Gy/min.

Chemicals

We used the following inhibitors: PD98059 against MEK1 at a concentration of 50 µM, U0126 against MEK1 and MEK2 at a concentration of 25 µM, MK-2206 2 HCl against AKT1/2/3 at a concentration of 5 µM and SB203580 against p38 MAP kinase at a concentration of 10 µM (all from Selleck Chemicals, Houston, TX, USA).

Wound-healing assay

We performed a wound-healing assay to measure cell migration. Approximately 1 x 10^6 cells were seeded in 6-well plates and incubated for 24 h for formation of a confluent monolayer. On the next day, the monolayer was wounded as homogenously as possible using a 200 µl pipette tip, washed with 1× DPBS (Gibco® Life Technologies, Carlsbad, CA, USA) and then pretreated with the inhibitor PD98059, U0126, MK-2206 2HCl or SB203580. After 1 h of incubation, irradiation was performed with 2 Gy and 10 Gy. Microscopic photos were obtained of the exact same area immediately (0 h) and at 10 h after irradiation to monitor the movement of the cells using a Leica DMI 6000B microscope, a Leica DFC425 C camera and Leica Application Suite Software V3.8. To analyze cell migration, we examined the decrease in the wounded area after 5 and 10 h using Adobe Photoshop CS5 and the following formula:

$$A(\%) = 100\% \times \frac{P2 - P1}{PG}$$

where A indicates the area of overgrowth in the picture during a certain period of time, PG is the total pixel number of the photograph, P1 is the pixel number of the scratch at the first time point, and P2 is the pixel number at the second time point.

Western blot analysis

For protein analysis, cells were grown to 70% confluence in 10-cm tissue culture dishes. At 24 h, 48 h, 72 h or 96 h after irradiation and/or additional pretreatment with inhibitors, the cells were washed with ice-cold 1× DPBS and lysed with 500 µl of cell lysis buffer. The buffer contained 1× Cell Lysis Buffer (Cell Signaling, Danvers, USA), 1 mM PMSF (Carl Roth, Karlsruhe, Germany) and 1× Protease Inhibitory Cocktail (Cell Signaling). The lysis buffer (10×) (Cell Signaling) included 20 mM Tris-HCl (pH 7.5), 150 mM NaCl, 1 mM Na_2EDTA, 1 mM EGTA, 1% Triton, 2.5 mM sodium pyrophosphate, 1 mM beta-glycerophosphate, 1 mM Na3V04, and 1 µg/ml leupeptin. Next, the cells were scraped off of the culture dishes, pipetted into 1.5-ml microtubes, incubated on ice and centrifuged at 4°C and 10,000 rpm for 15 min to isolate the soluble protein fraction. The clarified lysate was frozen at -20°C until use in the Bradford assay.

The Bradford assay was used to ensure for equal protein concentrations to verify that equal amounts were loaded per lane on an SDS-PAGE.

Equal protein concentrations (15 µg) were separated for 3 h at 120 V using an SDS-PAGE (Blotting System Mini-PROTEAN® Tetra System and PowerPac™ HC from Bio-Rad Laboratories, Munich, Germany) in a Tris-glycine running buffer. The densities of the running gels ranged from 7.5%-12.5%, and the stacking gels possessed a density of 5%. The proteins were then transferred to a polyvinylidene fluoride (PVDF) membrane (Merck Millipore, Darmstadt, Germany) using a Trans-Blot® SD Semi Dry Transfer Cell (Bio-Rad Laboratories, Munich, Germany) at 225 mA for 80 min. A solution containing 5% non-fat dry milk in 1× TBS and 0.1% Tween-20 was used to block unspecific binding sites. The membranes were then incubated with the primary antibodies in 1× TBS + 0.1% Tween-20 for 12 h at 4°C, washed and incubat-

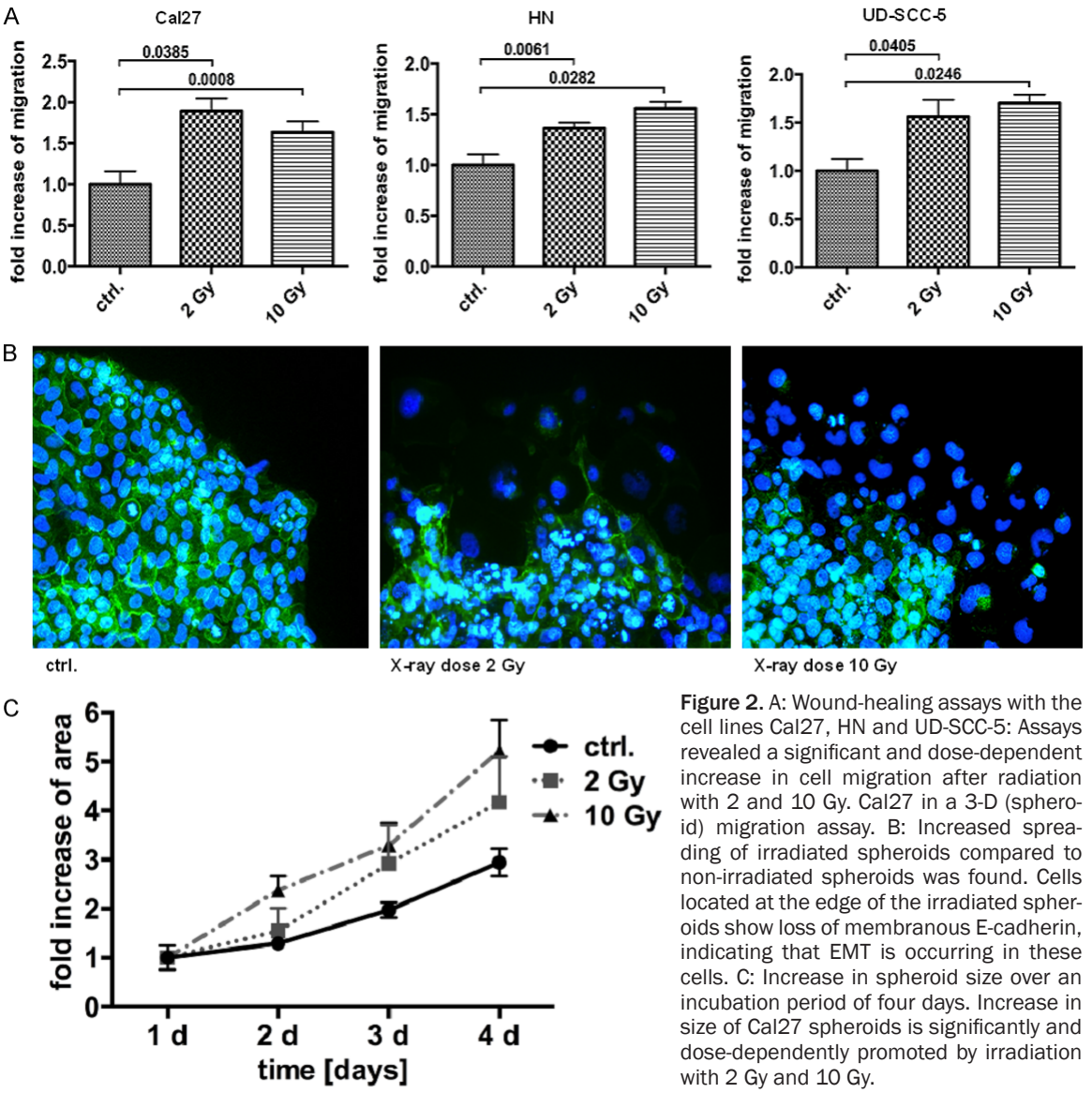

Figure 2. A: Wound-healing assays with the cell lines Cal27, HN and UD-SCC-5: Assays revealed a significant and dose-dependent increase in cell migration after radiation with 2 and 10 Gy. Cal27 in a 3-D (spheroid) migration assay. B: Increased spreading of irradiated spheroids compared to non-irradiated spheroids was found. Cells located at the edge of the irradiated spheroids show loss of membranous E-cadherin, indicating that EMT is occurring in these cells. C: Increase in spheroid size over an incubation period of four days. Increase in size of Cal27 spheroids is significantly and dose-dependently promoted by irradiation with 2 Gy and 10 Gy.

ed with an HRP-linked secondary antibody in 5% non-fat dry milk in 1× TBS and 0.1% Tween-20 for 1 h at room temperature. Next, the membranes were washed and incubated in Thermo Scientific™ Pierce™ ECL Western Blotting Substrate (Fisher Scientific, Waltham, MA, USA) for 1 min. Immunoreactivity was visualized by ChemiDoc XRS+ with Image Lab™ Software (Bio-Rad Laboratories, Munich, Germany).

Antibodies

We used primary antibodies against AKT (Cell Signaling), p-AKT Ser473 (Cell Signaling), ERK1/2 (Cell Signaling), p-ERK1/2 Thr202/Tyr204 (Cell Signaling), p38 MAPK (D13E1), p-p38 MAPK Thr180/Tyr182 (D3F9), GSK3β (27C10) (Cell Signaling), p-GSK3β Ser9 (5B3) (Cell Signaling), p-GSK3β Thr390 (Cell Signaling), mTOR (Cell Signaling), p-mTOR Ser2448 (XP-D9C2) (Cell Signaling), p70S6 kinase (Cell Signaling), p-p70S6 kinase Thr389 (Cell Signaling), 4EBP1 (Cell Signaling), p-4EBP1 Ser65 (Cell Signaling), FAK (D2R2E) (Cell Signaling), p-FAK Tyr297 (Becton Dickinson, Franklin Lakes, USA), β-catenin (6B3) (Cell Signaling), p-β-catenin Ser33/37 (Cell Signaling), paxillin (Cell Signaling), p-paxillin Tyr118 (Cell Signaling), CD29 integrin β1 (Becton Dickinson), CD104 integrin β4 (Becton Dickinson), Sin1 (D7G1A) (Cell Signaling), p-Sin1 Ser385 (11D1.1) (Merck Millipore), phosphothreonine (20H6.1) (Merck Millipore), tubulin (Sigma Aldrich, St. Louis, MO, USA) and

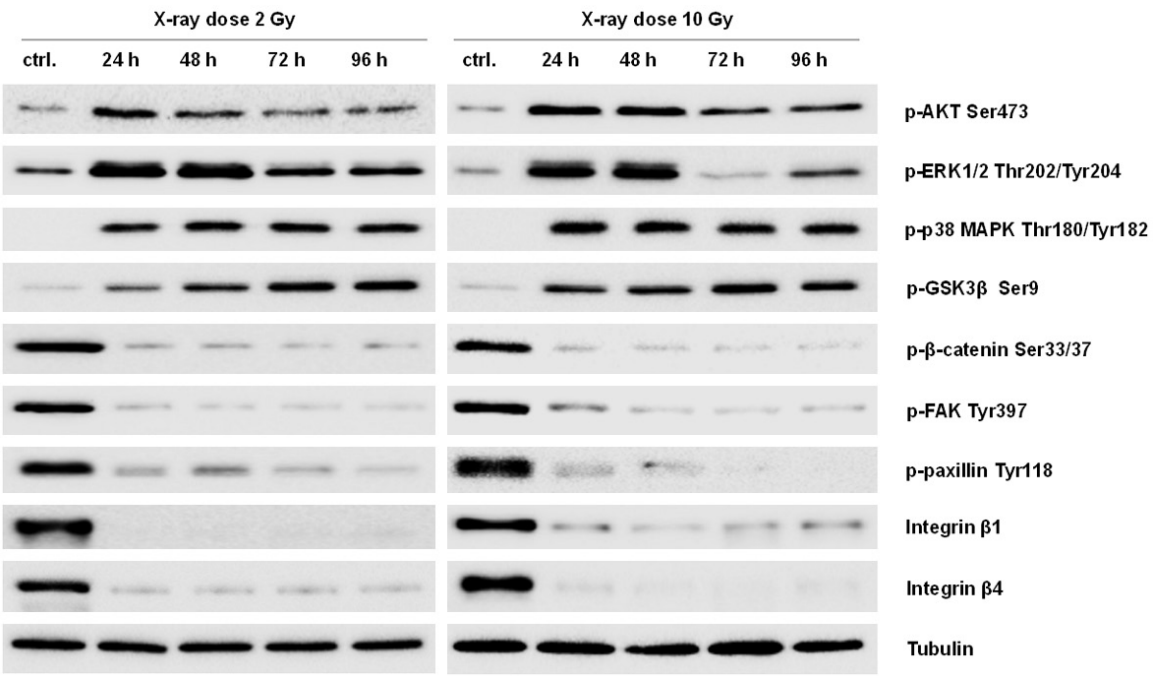

Figure 3. Irradiation-dependent intracellular signaling in Cal27 cell line: Western blots show permanent phosphorylation of AKT, ERK and stress-induced p38 MAPK, which all remained activated at the same levels for 96 h after irradiation. GSK3β, which appears unphosphorylated under control conditions, also becomes phosphorylated by irradiation. To assess the inactivation of GSK3β by phosphorylation, we examined its targets, including β-catenin, FAK, paxillin and integrins, and found reductions in protein phosphorylation for β-catenin (Ser33/37), FAK (Tyr397), and paxillin (Tyr118) and the loss of integrins β_1 and β_4, indicating GSK3β inactivation.

E-cadherin 24E10 (Cell Signaling). As secondary antibodies, anti-rabbit HRP-linked IgG (Cell Signaling) and anti-mouse HRP-linked IgG (Cell Signaling) were used. We used a Cy3® goat anti-rabbit (H+L) secondary antibody for immunofluorescence (Invitrogen, Carlsbad, CA, USA).

Immunoprecipitation (IP)

Protein lysates were obtained as described for the Western blot analysis. For immunoprecipitation, we used a Catch and Release® v2.0 Kit (Merck Millipore) according to the manufacturer's instructions. The Bradford assay was used to identify the amount of lysate containing 500 µg of protein. For IP, we used a primary antibody against Sin1 (D7G1A) (Cell Signaling). For Western blot analysis, we used anti-phosphothreonine and anti-rabbit HRP-linked IgG antibodies (Cell Signaling).

3D-cell culture: generating spheroids

Cal27 cells were used to generate spheroids with a Gravity PLUS™ Kit (InSphero, Schlieren, Switzerland). A total of 2.5×10^3 cells/spheroid were incubated in a Gravity PLUS™ System for three days, transferred to a Gravity TRAP™ System (InSphero) and incubated for one more day. Next, the generated microtissues were collected from the Gravity TRAP™ system and transferred to an ibidi 8-well µ-slide coated with ibiTreat (ibidi, Martinsried, Germany). After incubation for one day to allow for the microtissues to settle, they were exposed to irradiation with a single dose of 2 Gy or 10 Gy. Microscopic pictures of the spheroids were captured daily for 5 days to measure the migration of the cells out of the microtissues into the 8-well coated slides using a Leica DMI 6000B microscope, Leica DFC425 C camera and Leica Application Suite Software V3.8.

Immunofluorescence with E-cadherin

At 6 days after irradiation, the spheroids on the µ-slides were fixed for 20 min with 200 µl of 4% formaldehyde/1× DPBS, and they were then washed twice for 5 min each with 1× DPBS. The slides were incubated with 200 µl of 50 mM NH_4Cl/1× DPBS, washed 3 times for 2 min each with 1× DPBS and blocked with 200 µl of 5% normal goat serum/1× DPBS for 30 min.

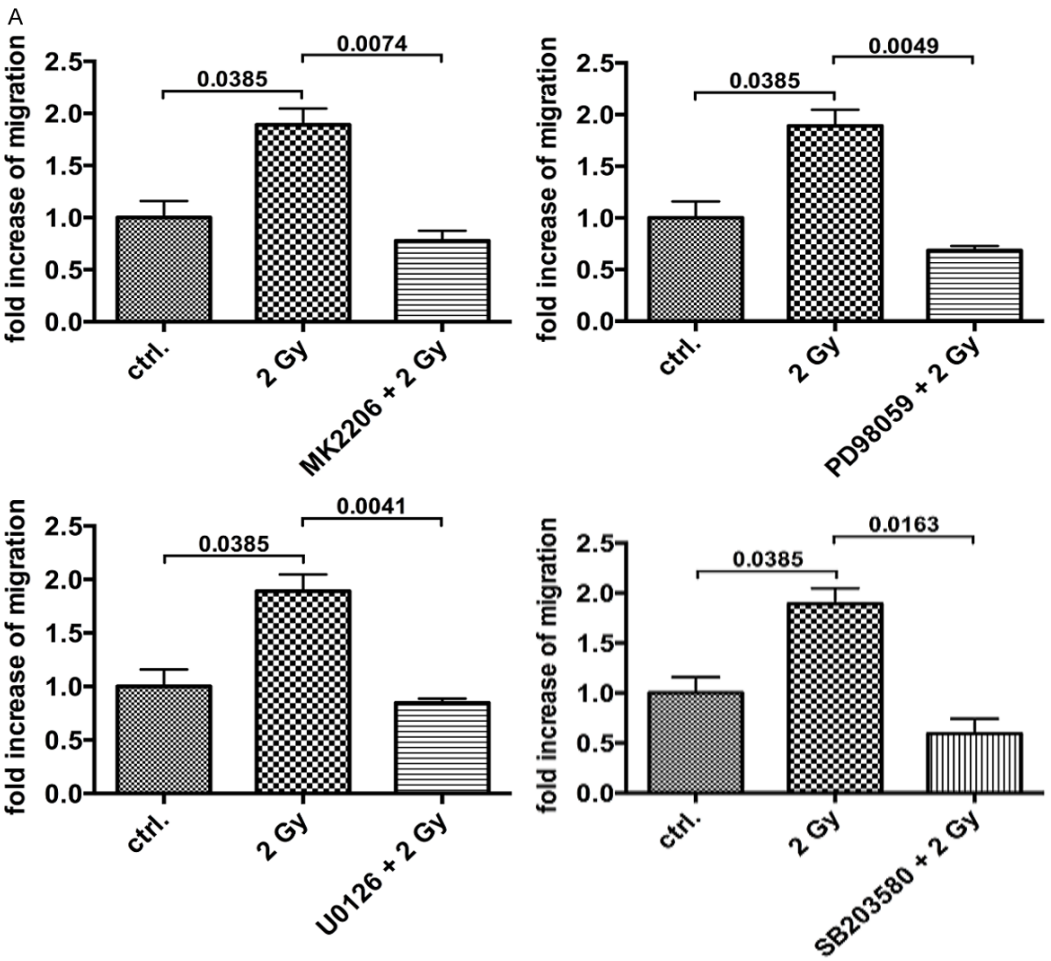
A
fold increase of migration
0.0385
0.0074
0.0049
0.0041
0.0163
ctrl.
2 Gy
MK2206 + 2 Gy
PD98059 + 2 Gy
U0126 + 2 Gy
SB203580 + 2 Gy

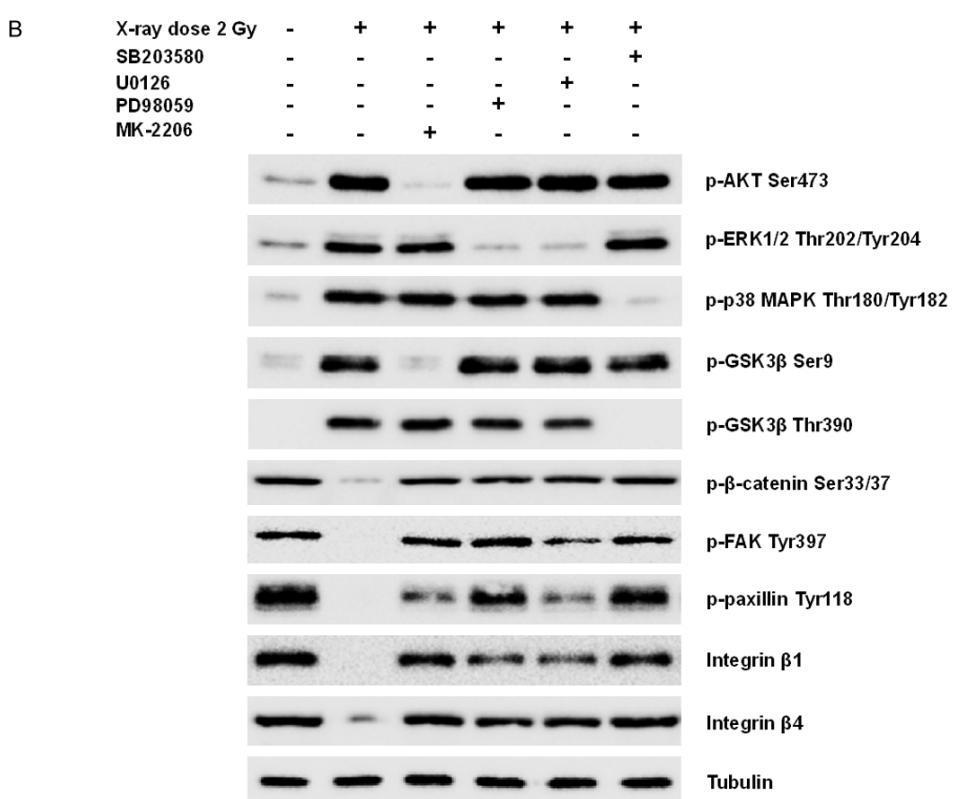
B
X-ray dose 2 Gy
SB203580
U0126
PD98059
MK-2206
p-AKT Ser473
p-ERK1/2 Thr202/Tyr204
p-p38 MAPK Thr180/Tyr182
p-GSK3β Ser9
p-GSK3β Thr390
p-β-catenin Ser33/37
p-FAK Tyr397
p-paxillin Tyr118
Integrin β1
Integrin β4
Tubulin

Figure 4. A: Wound-healing assays with Cal27 cells: Radiation-induced migration could be reduced to at least control levels by each of the following inhibitors: MK-2206 against AKT1/2/3, SB203580 against p38 MAPK, U0126 against MEK1/2, and PD98059 against MEK1. B: Intracellular signaling in Cal27 cells following irradiation and specific molecular inhibition: GSK3β was inactivated by phosphorylation via phosphorylated AKT, ERK and p38 MAPK. After inhibition of either AKT, ERK or p38 MAPK, we detected de-phosphorylation of GSK3β. Also GSK3β reactivation could be indirectly shown via downstream targets of GSK3β, such as β-catenin. Increases in p-β-catenin Ser33/37, FAK (Tyr397), paxillin (Tyr118) and integrins β_1 and β_4 after inhibition with each inhibitor are obvious, indicating regained GSK3β function.

Subsequently, a primary antibody against E-cadherin 24E10 (Cell Signaling) (diluted 1:200 with Antibody Diluent, Dako, Hamburg, Germany) was added, and the slides were incubated at 4°C overnight. On the next day, the slides were washed 3 times with 1× DPBS for 5 min each and incubated with a Cy3® goat anti-rabbit (H+L) secondary antibody (Invitrogen) (diluted 1:100 with Antibody Diluent) at room temperature for 1 h. Next, they were re-washed 3 times with 1× DPBS for 5 min each. The slides were stained with Hoechst 33342 dye (Thermo Scientific) for 5 min to visualize the nuclei. After washing with 1× DPBS, we captured images of the stained spheroids with a Leica DMI 6000B microscope, Leica DFC425 C camera and Leica Application Suite Software V3.8.

Statistics

Statistical analyses of the results from the *in vitro* experiments were performed using Prism Graph Pad 5.0 software. The whole analyses were repeated n = 3 times using triplets. Assuming normally distributed data, all of the hypotheses were tested with a t-test. We compared the separate treatments and the untreated control for statistical significance with a t-test (p-values < 0.05).

Results

Radiation induces tumor migration and down-regulation of membranous E-cadherin

First, we performed a wound-healing assay using three different HNSCC cell lines (Cal27, HN and UD-SCC-5) that we have previously used in different studies and examined the effects of irradiation on their migration capacities [6, 20]. In all of the cell lines, we observed dose-dependent, radiation-induced, and significantly enhanced cell migration at 10 h after irradiation with single doses of 2 Gy and 10 Gy (**Figure 2A**).

To extend the analysis to a more *in vivo*-like system, we investigated the effects of irradiation on HNSCC microtissues and established 3-dimensional spheroid growth of Cal27 tumors. After irradiation of ibiTreat-coated µ-slides (ibidi®, Martinsried, Germany) with 2 Gy and 10 Gy, we quantified spheroid sizes and evaluated 3-D growth integrity. We found increased cell dissociation and spreading in the irradiated spheroids compared to the non-irradiated spheroids (**Figure 2B**, **2C**).

Because decreased E-cadherin expression has been associated with reduced tissue differentiation and tumor progression (higher rate of lymph node metastasis) in HNSCC [21], we stained fixed spheroids (4% paraformaldehyde) for E-cadherin. Cells located at the edge of the irradiated spheroids showed a loss of membranous E-cadherin expression and altered cell morphology (**Figure 2B**).

Radiation-induced combined ERK, AKT, and p38 MAPK activation results in phosphorylation/inactivation of GSK3β

We have previously shown that radiation-induced EGFR phosphorylation correlates with enhanced cell migration [4-6]. Consistently, Schmidt-Ullrich et al. have described EGFR activation in squamous cell carcinoma immediately following irradiation [22]. Here, we evaluated the downstream signaling of EGFR at specific time points after irradiation. To this end, we sequentially analyzed protein levels within a period of 24 to 96 h after irradiation. We found the constitutive activation of the EGFR-dependent downstream targets AKT and ERK and induction of the stress-induced p38 MAPK enzyme, which all remained activated at the same levels for 96 h after irradiation (**Figure 3**).

GSK3β, which appears unphosphorylated under control conditions, also becomes phosphorylated by irradiation. To assess the inactivation of GSK3β by phosphorylation, we examined its targets, including β-catenin, FAK, paxil-

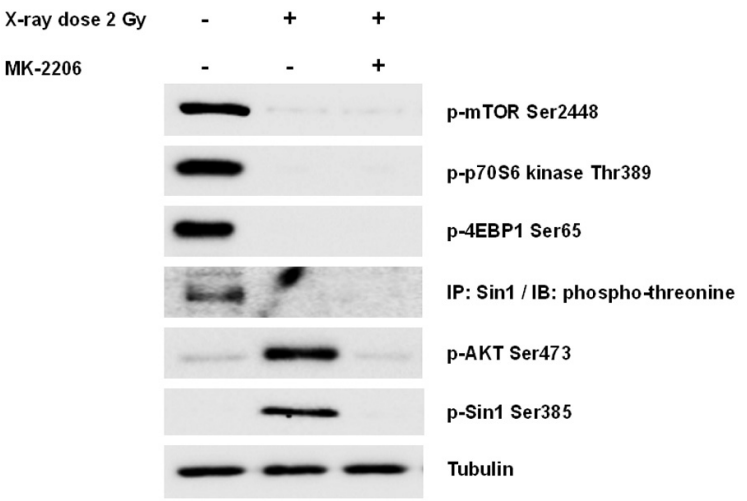

Figure 5. Irradiation-dependent AKT signaling leading to Sin1 phosphorylation in the cell line Cal27: Despite AKT-activation, mTOR phosphorylation at Ser2448 is reduced upon irradiation. Additionally, p70S6 kinase and 4EBP1 are inhibited. Sin1 was extracted via immunoprecipitation, and its threonine phosphorylation was analyzed. No Sin1 threonine phosphorylation was detectable under irradiation, while phosphorylation of AKT at Ser473 and phosphorylation of Sin1 at Ser385 were found.

lin and integrins, and found reductions in protein phosphorylation for β-catenin (Ser33/37), FAK (Tyr397), and paxillin (Tyr118) and the loss of integrins β_1 and β_4, indicating GSK3β inactivation (**Figure 3**).

GSK3β inactivation correlates with radiation-induced migration

Next, we evaluated to what extent the direct inhibition of EGFR-related downstream pathways reduces tumor cell migration in vitro. To this end, we treated Cal27 cells with the AKT1/2/3 inhibitor MK-2206 (5 μM), the p38 MAPK inhibitor SB203580 (10 μM), the MEK1/2 inhibitor U0126 (25 μM), and the MEK1 inhibitor PD98059 (50 μM) in a wound-healing assay. We found that radiation-induced migration was reduced at least to the control level following application of each of the inhibitors. Conclusively, the exclusive inhibition of just one of these upregulated pathways was sufficient to reduce radiation-induced migration in HNSCC (**Figure 4A**).

GSK3β was inactivated by phosphorylation via phosphorylated AKT, ERK and p38 MAPK. After inhibition of either AKT, ERK or p38 MAPK, we detected de-phosphorylation of GSK3β at Ser9 following treatment with MK-2206 and at Thr390 after treatment with SB203580 according to the different positions of phosphorylation. Due to the lack of commercial GSK3β and Thr43 antibodies, the impact of ERK inhibition on GSK3β reactivation could only be indirectly shown via downstream targets of GSK3β, such as β-catenin. Increases in p-β-catenin Ser-33/37, FAK (Tyr397), paxillin (Tyr118) and integrins β_1 and β_4 after inhibition with each inhibitor are obvious, indicating regained GSK3β function (**Figure 4B**).

Irradiation-dependent AKT signaling leading to Sin1 phosphorylation

In the HNSCC cell line Cal27, we found mTOR phosphorylation at Ser2448 under control conditions (without irradiation). Under radiation mTOR phosphorylation at Ser2448 is reduced, despite AKT-activation. Additionally, p70S6 kinase and 4EBP1 are inhibited. As AKT phosphorylation at Ser 473 was recently linked with a mTORC2 stabilization via dephosphorylation of Sin1 at its threonine residues [23], we extracted Sin1 via immunoprecipitation and analyzed its threonine phosphorylation. No Sin1 threonine phosphorylation was detectable under irradiation, while phosphorylation of AKT at Ser473 and phosphorylation of Sin1 at Ser385 were found (**Figure 5**).

Discussion

Local or regional recurrence at a previously irradiated tumor site is common in HNSCC. Recently it has been demonstrated that sublethal irradiation promotes enhanced tumor cell migration [4-6], which could be responsible for regional recurrence. Here, we investigated the effects of irradiation on EGFR dependent pathways with the option to reduce cell migration by inhibition of specific intracellular targets.

GSK3β as a critical player for radiation-induced migration

With our experiments we were able to identify a radiation-induced cell migration and to clearify its molecular mechanisms, especially attribut-

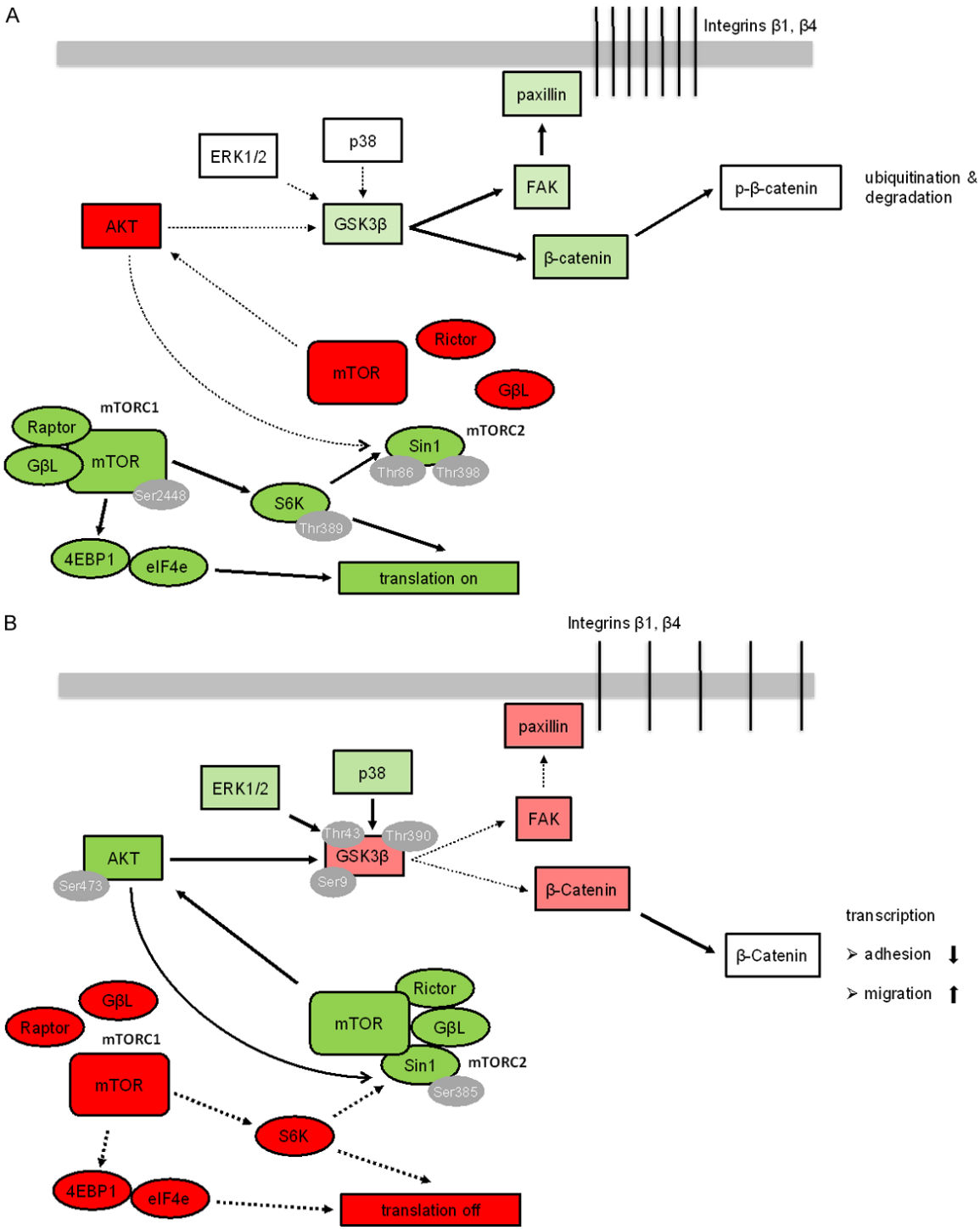

Figure 6. A mechanistic model for irradiation-dependent and GSK3β-related signaling in HNSCC cells: Activated and inactivated molecules are displayed in green and in red, respectively. A: In non-irradiated HNSCC tumor cells, mTOR is phosphorylated at Ser2448, which stabilizes mTORC1 and leads to phosphorylation of p70S6 kinase. Activated p70S6 kinase phosphorylates Sin1 at Thr86 and Thr398, thus destabilizing mTORC2 with subsequent dissociation and de-phosphorylation of AKT at Ser473. Because inactivation of either AKT, ERK, or p38 MAPK is sufficient for reactivating GSK3β function, β-catenin and FAK were able to be phosphorylated. B: In contrast, radiation leads to a loss of mTOR phosphorylation at Ser2448 and of p70S6K at Thr389, resulting in dephosphorylation of Sin1 at its threonine residues. Dephosphorylated Sin1 stabilizes mTORC2, mediating AKT activation at Ser473. This AKT activation leads to phosphorylation of Sin1 at Ser385 via a feedback loop. The AKT pathway is (besides the ERK and p38 MAPK pathways) one of the three pathways that collectively mediate tumor cell migration via GSK3β inhibition.

ing GSK3β a key role in cell migration. We demonstrated a dose-dependent, radiation-induced, and significantly enhanced cell migration. Also, using a more *in vivo*-like system the 3-dimensional spheroid growth of Cal27 tumors, we observed increased cell dissociation and spreading in the irradiated spheroids (**Figure 2A-C**).

Because E-cadherin expression has been associated with reduced tissue differentiation, enhanced invasiveness, EMT [18], and tumor progression (higher rate of lymph node metastasis) in HNSCC [21], we stained the spheroids. We found, that cells located at the edge of the irradiated spheroids had a loss of membranous E-cadherin expression. This finding can be considered to be indicative of EMT (**Figure 2B**). Overall, irradiation applied to growing spheroid cells appeared to enhance their migratory potential. This observation is consistent with the results revealed by monolayer wound-healing assays.

Western blot assays showed constitutive activations of the EGFR-dependent downstream targets AKT and ERK and induction of the stress-induced p38 MAPK enzyme (**Figure 3**). Increased ERK activity upon irradiation in HNSCC has been previously described elsewhere [24], and p38 MAPK is known to be activated via environmental stress e.g., irradiation [25]. These three pathways have been shown to control GSK3β activity [11, 13, 14]. As a marker for GSK3β activity, we used the β-catenin protein level. Activated non-phosphorylated GSK3β is able to phosphorylate β-catenin at Ser33/37, resulting in the proteasomal degradation of β-catenin. Here, we showed that combined radiation-induced ERK, AKT, and p38 MAPK activation was required to entirely phosphorylate and thereby to inactivate GSK3β in HNSCC. Under irradiation, the level of phosphorylated β-catenin at Ser33/37 was markedly reduced, suggesting a prevalence of inhibited GSK3β (**Figure 3**).

Next, we found that radiation-induced migration was reduced at least to the control level following application of each of the inhibitors MK-2206, SB203580, U0126, and PD98059. Conclusively, the exclusive inhibition of just one of these upregulated pathways was sufficient to reduce radiation-induced migration in HNSCC (**Figure 4A**).

In the HNSCC cell lines, GSK3β seemed to be capable of maintaining its control over cell migration unless AKT, p38 MAPK and ERK were collectively activated. Subsequently, the inactivation of either AKT, MEK/ERK, or p38 MAPK was sufficient to reactivate GSK3β function and thus increase p-β-catenin Ser33/37 protein levels (**Figure 4B**). GSK3β is not only known to affect tumor cell migration via β-catenin phosphorylation but also via the targeting of cell adhesion molecules, such as FAK and paxillin [19]. Irradiated cells showed losses of FAK (Tyr397) and paxillin (Tyr118) phosphorylation, and simultaneously, markedly diminished integrin β_1/β_4 expression (**Figure 3**). In contrast, reactivation of GSK3β by one of the EGFR pathway inhibitors led to enhanced FAK and paxillin phosphorylation and an increase in integrin β_1/β_4 expression, reaching the levels observed in the untreated (control) cells (**Figure 4B**). Hence, FAK and paxillin functions are apparently related to inhibited cell motility, which is compatible with increased HeLa cell motility following a loss of FAK or paxillin expression [26]. Moreover, Lu et al. have reported an association of EGFR overexpression and tyrosine dephosphorylation of FAK with decreased FAK activity followed by increased motility and invasion in HNSCC [27]. Consistently, we found that FAK phosphorylation was regulated by EGFR downstream signaling via AKT, ERK, and p38 MAPK, which in turn affected cell migration via GSK3β. Inhibition of GSK3β was associated with non-phosphorylated FAK and paxillin, while its activation led to phosphorylation of FAK and paxillin (**Figures 3**, **4B**). AKT and ERK are downstream targets of EGFR, indicating that the downregulation of FAK under EGF stimulation, which has been described previously by Lu et al., may be mediated via GSK3β. Moreover, GSK3β appeared to indirectly impact integrin β_1/β_4 expression. Histological analysis revealed the strong correlation of reduced integrin β_4 and nodal metastases in HNSCC patients [28]. Reduced β_1 integrin expression is predominantly found in poorly differentiated lesions [29]. Overall, loss of integrins is apparently connected with higher migratory capacity in HNSCC.

Radiation causes a positive feedback loop between AKT and mTORC2

In the HNSCC cell line, we found mTOR phosphorylation at Ser2448 under control condi-

tions (without irradiation), which stabilized mTORC1 and led to phosphorylation of p70S6 kinase at Thr389 (**Figure 5**). Liu et al. have previously reported that p70S6 kinase phosphorylates Sin1 at Thr86 and Thr398 and thus destabilizes mTORC2, resulting in its subsequent dissociation [23] (**Figure 6A**).

Although activated AKT is usually linked to enhanced mTORC1 activity and protein biosynthesis, we found dephosphorylated mTOR during increased AKT activation throughout irradiation. We have previously reported an observation of only a transient EGFR activation after irradiation [6]. However, AKT activation as shown here was observed over a period of 96 h (**Figure 3**). To facilitate data analysis, we analyzed Sin1 via immunoprecipitation and examined its extent of threonine phosphorylation. Dephosphorylated Sin1 at Thr86 and Thr398 is known to stabilize mTORC2, resulting in AKT (Ser473) phosphorylation [30]. Concordantly, we identified a loss of the threonine phosphorylation of Sin1. In addition, we found that irradiation resulted in phosphorylation of AKT at Ser473. This AKT (Ser473) phosphorylation was associated with phosphorylated Sin1 at Ser385. In contrast, inhibition of AKT with MK-2206 (5 μM) led to a loss of Sin1 (Ser385) phosphorylation (**Figure 5**) suggesting that Sin1 is dircetly or targeted by AKT at its Ser385 which affects mTORC2. This interaction was only possible when mTORC2 was stabilized and when Sin1 was not phosphorylated at its threonine residues by p70S6 kinase. These results suggest that irradiation triggered a feedback loop between AKT and Sin1 through a stabilized mTORC2 complex without EGFR involvement (**Figure 6B**).

Based on these data, we postulate the following model (**Figure 6**): Under radiation, dephosphorylated mTOR and p70S6 kinase induce dephosphorylation of Sin1 at its threonine phosphorylation sites. This provokes stabilization of mTORC2 with activated AKT. AKT is constitutively activated through a positive feedback loop, phosphorylating Sin1 at Ser385. The activation of AKT and the radiation-induced activation of ERK and p38 MAPK ultimately lead to the inactivation of GSK3β and dephosphorylation of the GSK3β targets FAK and β-catenin, contributing to increased cell migration.

Summary

Our findings indicate that irradiation contributes to a higher migratory capacity of HNSCC cells via different mechanisms, as follows: first, irradiation leads to the downregulation of membranous E-cadherin during EMT. Second, irradiation causes an upregulation of AKT/ERK/p38 MAPK phosphorylation/activation, consequently resulting in reduced GSK3β activity. Moreover, irradiation causes reduced paxillin and FAK phosphorylation and a loss of integrin β_1/β_4 expression, which is most likely mediated by attenuated GSK3β activity. Finally, AKT activity is maintained by stabilization of mTORC2 due to reduced mTORC1 and p70S6 kinase activity upon irradiation.

Conclusion

The combined activation of the AKT, p38 MAPK and ERK pathways by irradiation causes an inactivation of GSK3β kinase and results in enhanced tumor cell migration. In contrast, the exclusive inhibition of just one of these upregulated pathways is sufficient to reduce radiation-induced migration in HNSCC. These data indicate that pharmacological inhibition of one of these pathways targeting GSK3β could decrease radiation-induced cell migration in HNSCC, thus potentially reducing metastasis and locoregional recurrence in patients.

Disclosure of conflict of interest

None.

Address correspondence to: Dr. Anja Pickhard, Department of Otolaryngology Head and Neck Surgery, Technical University of Munich, Ismaninger Str. 22, Muenchen 81675, Germany. E-mail: a.pickhard@lrz.tum.de

References

[1] Ferlay J, Shin HR, Bray F, Forman D, Mathers C and Parkin DM. Estimates of worldwide burden of cancer in 2008: GLOBOCAN 2008. Int J Cancer 2010; 127: 2893-2917.

[2] Bose P, Brockton NT and Dort JC. Head and neck cancer: from anatomy to biology. Int J Cancer 2013; 133: 2013-2023.

[3] Blanchard P, Baujat B, Holostenco V, Bourredjem A, Baey C, Bourhis J, Pignon JP and MACH-CH Collaborative group. Meta-analysis of chemotherapy in head and neck

cancer (MACH-NC): a comprehensive analysis by tumour site. Radiother Oncol 2011; 100: 33-40.
[4] Wild-Bode C, Weller M, Rimner A, Dichgans J and Wick W. Sublethal Irradiation Promotes Migration and Invasiveness of Glioma Cells: Implications for Radiotherapy of Human Glioblastoma. Cancer Res 2001; 61: 2744-2750.
[5] Rappl A, Piontek G and Schlegel J. EGFR-dependent migration of glial cells is mediated by reorganisation of N-cadherin. J Cell Sci 2008; 121: 4089-4097.
[6] Pickhard AC, Margraf J, Knopf A, Stark T, Piontek G, Beck C, Boulesteix AL, Scherer EQ, Pigorsch S, Schlegel J, Arnold W and Reiter R. Inhibition of radiation induced migration of human head and neck squamous cell carcinoma cells by blocking of EGF receptor pathways. BMC Cancer 2011; 11: 388.
[7] Embi N, Rylatt DB and Cohen P. Glycogen Synthase Kinase-3 from Rabbit Skeletal Muscle Separation from Cyclic-AMP-Dependent Protein Kinase and Phosphorylase Kinase. Eur J Biochem 1980; 107: 519-527.
[8] Frame S and Cohen P. GSK3 takes centre stage more than 20 years after its discovery. Biochem J 2001; 359: 1-16.
[9] Mishra R. Glycogen synthase kinase 3 beta: can it be a target for oral cancer. Mol Cancer 2010; 9: 144.
[10] Iwai S, Yonekawa A, Harada C, Hamada M, Katagiri W, Nakazawa M and Yura Y. Involvement of the Wnt-β-catenin pathway in invasion and migration of oral squamous carcinoma cells. Int J Oncol 2010; 37: 1095-1103.
[11] Cross DAE, Alessi DR, Cohen P, Andjelkovich M and Hemmings BA. Inhibition of glycogen synthase kinase-3 by insulin mediated by protein kinase B. Nature 1995; 378: 785-789.
[12] Freudlsperger C, Burnett JR, Friedman JA, Kannabiran VR, Chen Z and Van Waes C. EGFR-PI3K-AKT-mTOR signaling in head and neck squamous cell carcinomas: attractive targets for molecular-oriented therapy. Expert Opin Ther Targets 2011; 15: 63-74.
[13] Thornton TM, Pedraza-Alva G, Deng B, Wood CD, Aronshtam A, Clements JL, Sabio G, Davis RJ, Matthews DE, Doble B and Rincon M. Phosphorylation by p38 MAPK as an alternative pathway for GSK3beta inactivation. Science 2008; 320: 667-670.
[14] Ding Q, Xia W, Liu JC, Yang JY, Lee DF, Xia J, Bartholomeusz G, Li Y, Pan Y, Li Z, Bargou RC, Qin J, Lai CC, Tsai FJ, Tsai CH and Hung MC. Erk associates with and primes GSK-3beta for its inactivation resulting in upregulation of beta-catenin. Mol Cell 2005; 19: 159-170.
[15] Deschenes-Simard X, Kottakis F, Meloche S and Ferbeyre G. ERKs in cancer: friends or foes? Cancer Res 2014; 74: 412-419.
[16] Klaus A and Birchmeier W. Wnt signalling and its impact on development and cancer. Nat Rev Cancer 2008; 8: 387-398.
[17] McCrea PD, Turck CW and Gumbiner B. A Homolog of the armadillo Protein in Drosophila (Plakoglobin) Associated with E-Cadherin. Science 1991; 254: 1359-1361.
[18] Peinado H, Portillo F and Cano A. Transcriptional regulation of cadherins during development and carcinogenesis. Int J Dev Biol 2004; 48: 365-375.
[19] Sun T, Rodriguez M and Kim L. Glycogen synthase kinase 3 in the world of cell migration. Dev Growth Differ 2009; 51: 735-742.
[20] Beck C, Piontek G, Haug A, Bas M, Knopf A, Stark T, Misslbeck M, Rudelius M, Reiter R, Brandstetter M and Pickhard A. The kallikrein-kinin-system in head and neck squamous cell carcinoma (HNSCC) and its role in tumour survival, invasion, migration and response to radiotherapy. Oral Oncol 2012; 48: 1208-1219.
[21] Schipper JH, Frixen UH, Behrens J, Unger A, Jahnke K and Birchmeier W. E-Cadherin Expression in Squamous Cell Carcinomas of Head and Neck: Inverse Correlation with Tumor Dedifferentiation and Lymph Node Metastasis. Cancer Res 1991; 51: 6328-6337.
[22] Schmidt-Ullrich RK, Valerie K, Fogleman PB and Walters J. Radiation-Induced Autophosphorylation of Epidermal Growth Factor Receptor in Human Malignant Mammary and Squamous Epithelial Cells. Radiat Res 1996; 145: 81.
[23] Liu P, Gan W, Inuzuka H, Lazorchak AS, Gao D, Arojo O, Liu D, Wan L, Zhai B, Yu Y, Yuan M, Kim BM, Shaik S, Menon S, Gygi SP, Lee TH, Asara JM, Manning BD, Blenis J, Su B and Wei W. Sin1 phosphorylation impairs mTORC2 complex integrity and inhibits downstream Akt signalling to suppress tumorigenesis. Nat Cell Biol 2013; 15: 1340-1350.
[24] Affolter A, Fruth K, Brochhausen C, Schmidtmann I, Mann WJ and Brieger J. Activation of mitogen-activated protein kinase extracellular signal-related kinase in head and neck squamous cell carcinomas after irradiation as part of a rescue mechanism. Head Neck 2011; 33: 1448-1457.
[25] Raingeaud J, Gupta S, Rogers JS, Dickens M, Han J, Ulevitch RJ and Davis RJ. Pro-inflammatory Cytokines and Environmental Stress Cause p38 Mitogen-activated Protein Kinase Activation by Dual Phosphorylation on Tyrosine and Threonine. J Biol Chem 1995; 270: 7420-7426.

[26] Yano H, Mazaki Y, Kurokawa K, Hanks SK, Matsuda M and Sabe H. Roles played by a subset of integrin signaling molecules in cadherin-based cell-cell adhesion. J Cell Biol 2004; 166: 283-295.
[27] Lu Z, Jiang G, Blume-Jensen P and Hunter T. Epidermal growth factor-induced tumor cell invasion and metastasis initiated by dephosphorylation and downregulation of focal adhesion kinase. Mol Cell Biol 2001; 21: 4016-4031.
[28] Eriksen JG, Steiniche T, Sogaard H and Overgaard J. Expression of integrins and E-cadherin in squamous cell carcinomas of the head and neck. APMIS 2004; 112: 560-568.
[29] Thomas GJ, Jones J and Speight PM. Integrins and Oral Cancer. Oral Oncology 1997; 33: 381-388.
[30] Jacinto E, Facchinetti V, Liu D, Soto N, Wei S, Jung SY, Huang Q, Qin J and Su B. SIN1/MIP1 maintains rictor-mTOR complex integrity and regulates Akt phosphorylation and substrate specificity. Cell 2006; 127: 125-137.